

1-1-2006

# AC/DC Power Systems with Applications in Future Human Habitat on Lunar and Mars Bases

Badrul H. Chowdhury

*Missouri University of Science and Technology*, [bchow@mst.edu](mailto:bchow@mst.edu)

Sabbir A. Hossain

James T. Lawrence

Sushant Barave

Follow this and additional works at: [http://scholarsmine.mst.edu/ele\\_comeng\\_facwork](http://scholarsmine.mst.edu/ele_comeng_facwork)



Part of the [Electrical and Computer Engineering Commons](#)

---

## Recommended Citation

B. H. Chowdhury et al., "AC/DC Power Systems with Applications in Future Human Habitat on Lunar and Mars Bases," *American Institute of Physics Conference Proceedings*, American Institute of Physics (AIP), Jan 2006.

The definitive version is available at <http://dx.doi.org/10.1063/1.2169195>

This Article - Conference proceedings is brought to you for free and open access by Scholars' Mine. It has been accepted for inclusion in Electrical and Computer Engineering Faculty Research & Creative Works by an authorized administrator of Scholars' Mine. This work is protected by U. S. Copyright Law. Unauthorized use including reproduction for redistribution requires the permission of the copyright holder. For more information, please contact [scholarsmine@mst.edu](mailto:scholarsmine@mst.edu).

# AC/DC Power Systems with Applications in Future Human Habitat on Lunar and Mars Bases

Badrul H. Chowdhury<sup>1</sup>, Sabbir A. Hossain<sup>2</sup>, James T. Lawrence<sup>2</sup>, Sushant Barave<sup>1</sup>

<sup>1</sup>Electrical & Computer Engineering Department, University of Missouri-Rolla, Rolla, MO 65409

<sup>2</sup>ISS Electrical Power System Team, Energy Systems Division - EP5, NASA Johnson Space Center,

Houston, TX 77058

573-341-6230, bchow@umr.edu

**Abstract.** As NASA readies itself for new space exploration initiatives starting with a human return to the Moon by the year 2020 eventually leading to human exploration of Mars, the requirements for a safe, efficient and comprehensive power system to support the exploration missions as well human habitat will become important issues to consider. Certain issues dealing with electric power generation and distribution on board Mars-bound vehicles and those on Lunar and Martian surfaces are described. The requirements for lightweight power generation dictates the use of a high frequency ac machine. Preliminary results of investigating the design of a permanent magnet synchronous machine is presented.

**Keywords:** Crew exploration vehicle, high frequency power generation, permanent magnet synchronous machine.

**PACS:** 84.50, 84.70.

## INTRODUCTION

NASA (NASA, 2004) envisions a human return to the Moon by the year 2020, in preparation for human exploration of Mars and other destinations. The vision has two specific initiatives:

Lunar Exploration:

- Begin robotic missions to the Moon by 2008, followed by a period of evaluating lunar resources and technologies for exploration
- Begin human expeditions to the Moon in the 2015 – 2020 timeframe

Mars Exploration:

- Conduct robotic exploration of Mars to search for evidence of life, to understand the history of the solar system, and to prepare for future human exploration.

Both initiatives will require NASA to develop and demonstrate power generation, propulsion, life support, and other key capabilities required to support more distant, more capable, and longer duration human and robotic exploration than ever done before. This paper describes the requirements for power generation and distribution for human habitat on lunar/Martian surface and provides a system-level design. Design details are provided for an ac generator at a higher than normal frequency. The paper discusses the critical issue of whether the generator should generate at constant or variable frequency. This will decide what type of generator to use – whether it is a synchronous machine, an asynchronous induction machine or a switched reluctance machine.

Fig. 1 shows the essential ingredients of a viable power system for future space applications. Low weight and high reliability are only two of the major constraints because of longer travel distances and mission-critical payload involved. In contrast, the requirements for terrestrial power systems are only a subset of those listed in Fig. 1. Therefore, the technological challenges in power systems for future space exploration are formidable and will require a careful study of what technology is available today and what needs to be developed before the vision can become a reality.

Mars-bound crew exploration vehicles present extra-ordinary challenges mainly because of the never-before-attempted human interplanetary travel involved as well as the need to transport some payload for creating a habitat on Mars. Because of the need for light weight on crew exploration vehicles, higher frequency ac generation at frequencies 400 ~ 1200 Hz as the fundamental frequency is a good option to explore. There is a wealth of literature

on application of 400 Hz systems in naval ships and the aerospace industry. Some of US Navy’s newest ships use 400 Hz, 3-phase nuclear power generation. The current state-of-the-art in aerospace power is 400 Hz, 115 V (line-neutral), at either variable frequency or constant frequency. Current aircraft electric power generation technology uses both the constant speed drive (CSD) and the variable speed constant frequency (VSCF) technology. The CSD is an engine mounted generator system complete with an electrical generator and a variable displacement pump that constantly adjusts the output shaft rotation to maintain 24,000 RPM regardless of the throttle setting of the engine.

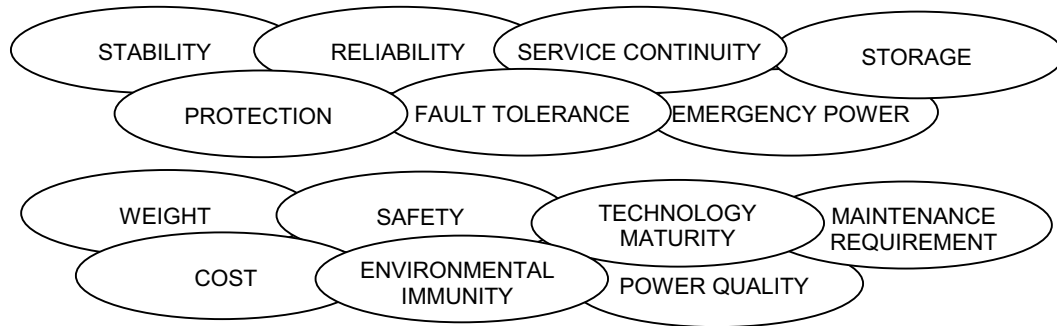


**FIGURE 1.** Considerations for Power Systems for Future Space Applications.

Unfortunately, some of the conditions for future explorations beyond LEO will be quite different. The fuel source will be different and the power system will be required to operate at higher voltage and power levels and for much longer durations without maintenance. Therefore, novel designs are required for the electric power generation system that will exhibit high power and energy densities. One such option is to re-design the permanent magnet machine – the current motor of choice for the hybrid electric vehicle industry.

### THE PERMANENT MAGNET GENERATOR

A permanent magnet machine topology is selected for final design and performance analysis. The requirements of the generator are listed below:

- High power density and energy density - this will ensure that the machine is compact, which is a major consideration, as the machine needs to be transported along with the vehicle.
- Relatively high electrical frequency resulting in reduced machine size.
- Low rotor loss causing less heating and in turn enhancing machine life.
- Low torque ripple (low cogging) and lower THD of flux results in a safer, interference-free operation.
- High thermal endurance and ability to operate in vacuum without extensive cooling requirement.

A conceptual block diagram of the overall generating system is depicted in the block diagram of Fig. 2. It gives a fair idea about the involvement of power electronic circuitry in the system.

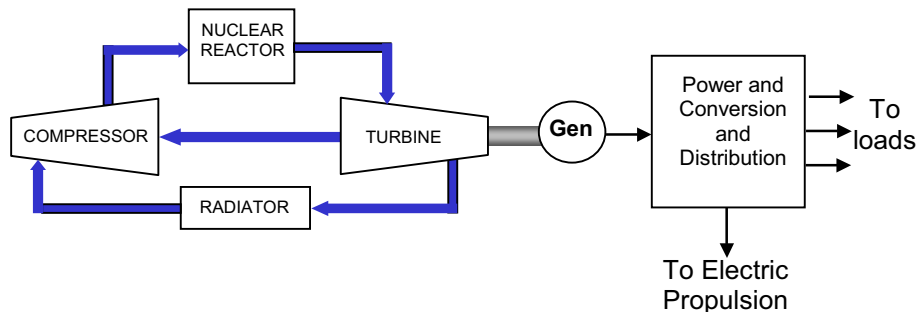


**FIGURE 2.** Conceptual Block Diagram of Space Nuclear System with Closed Brayton Cycle (CBC) Energy Conversion.

The permanent magnet generator is a synchronous machine where the rotor windings have been replaced with permanent magnets. This in turn reduces the copper losses in the machine. Iron losses form a larger portion of total losses in PM machines (Mi, 2005).. The permanent magnet generator is popular in automotive applications because

of its efficiency, reliability, high power density, and possibilities for high speed operating points. These qualities make it a very promising candidate for space application. These machines are becoming popular in view of their higher potential efficiencies, high power densities and the availability of high-energy permanent magnet materials (Trout, 2003), (Deshpande, 2003), (Ojo, 1997). Some advantages of the PM machine for space applications include:

- It can impart savings in machine weight and size
- Certain types of permanent magnet generators can result in improvement of power densities by almost a factor of 2, over induction machines (Huang, 1998).
- With proper design, the PM machine generally results in higher energy efficiency than any other type of rotating machine an equivalent power output.
- Absence of brushes, slip-rings, excitation windings, etc. result in decreased maintenance.

The axial flux PM machine is one variation of the traditional PM machine. This type of machine is discussed in (Sahin, 2001), (Caeicchi, 1998), and (Henselman, 1994). This paper will only concentrate on the radial flux type PM machines. A cross-sectional view of such a machine is shown in Fig. 3.

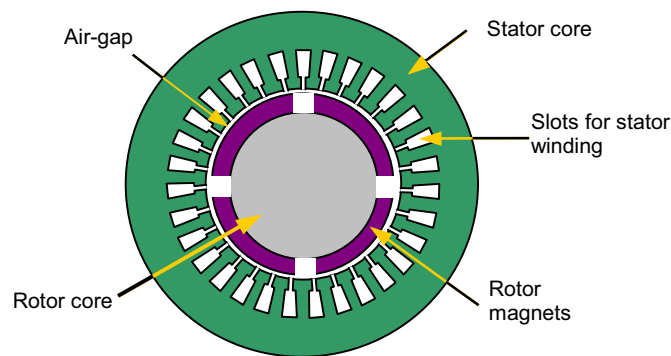


**FIGURE 3.** Cross-Sectional View of a Radial Flux Permanent Magnet Synchronous Machine.

### Design Parameters

Many parameters are involved in the design of an electrical machine. There are no definite guidelines for the procedure. Hence one has to rely heavily on some assumptions as a starting point in the design. It is absolutely necessary to assign constant values to some of the parameters and then determine the remaining part of the design (Qu, 2004). Again these fixed parameters may vary as per the design purpose. Common fixed parameters will be rated speed, torque, power output, permitted volume and related geometrical as well as electrical properties of materials. The magnetic properties desired and the electrical quantities dictate the geometrical parameters. After surveying a number of permanent magnet machines of a wide range of ratings for high frequency operation (Dravid, 2003), (Mi, 2005), (Magnussen, 2004), (Nagorny, 2004), a specific size of the machine is assumed as a starting point. Thus, the axial length, rotor outer radius, stator outer radius are assumed to be fixed. By initially specifying these dimensions, the design equations follow in a straightforward fashion and no iteration is required to find the solution to the design problem. The design is started from the basic geometrical constraints and the magnetic circuit describing the flux flow.

Loss calculation is one aspect of machine design which has numerous approaches (Mi, 2005), (Algen, 2003), (Magnussen, 2004). Apart from the loss component calculations, the design equations used are based on the processes and analysis in (Henselman, 1994) and (Hendershot, 1994). Radial flux topology is considered at the beginning, as it is the most widely available for future testing purpose.

Geometrical and constructional details such as number of phases, magnet poles, slots per phase, etc. are also classified as fixed parameters. By making a certain assumptions about the properties of the materials, we can proceed with the design procedure. Use of other materials will affect the entire machine performance, but going through the design procedure once, gives an idea of impact of the material properties on the entire design. The fixed parameters are listed in Table 1.

### Geometric parameters

Using the fixed parameters, the various radii associated with the machine are identified as follows:

The stator outer radius is calculated from the inner radius and the back iron width. This further leads to the rotor outer radius. From the angular pole pitch one can find out the pole pitch at inner stator surface as,

$$\tau_p = R_{si} \theta_p \quad (1)$$

where the angular pole pitch is,  $\theta_p = \frac{2\pi}{N_m}$ .

Coil Pitch at Stator Inner Radius is given by:

$$\tau_c = \alpha_p \tau_p \quad (2)$$

where  $\alpha_p = \frac{\tau_c}{\tau_p} = \text{int} \left[ \frac{(N_{spp})}{N_{spp}} \right]$

**TABLE 1.** The Fixed Parameters of the Permanent Magnet Synchronous Machine.

| Parameter  | Description   | Parameter     | Description                    |
|------------|---|---------------|--------------------------------|
| $P$        | Power (Hp)  | $R_{ro}$      | Rotor outside radius (m)       |
| $f$        | Operating frequency (Hz)                            | $L$           | Motor axial length (m)         |
| $E_{\max}$ | Maximum EMF (V)                                     | $k_{st}$      | Lamination stacking factor     |
| $J_{\max}$ | Maximum slot current density (A/m <sup>3</sup> )    | $\rho_{bi}$   | Steel mass density             |
| $N_{ph}$   | Number of phases                                    | $\rho$        | Conductor resistivity          |
| $N_m$      | Number of magnet poles                              | $k_{cp}$      | Conductor packing factor       |
| $N_{sp}$   | Number of slots per pole phase<br>$N_{sp} \geq N_m$ | $\alpha_m$    | Magnet fraction                |
| $g$        | Air gap length (m)                                  | $B_r$         | Magnet remanence (T)           |
| $l_m$      | Magnet length (m)                                   | $\mu_R$       | Magnet recoil permeability     |
| $R_{so}$   | Stator outside radius (m)                           | $B_{\max}$    | Maximum steel flux density (T) |
|            |   | $w_s$         | Slot opening (m)               |
|            |   | $\alpha_{sd}$ | Shoe depth fraction            |

This is the expression for the pitch factor. When  $N_{spp}$  is an integer, then pitch factor is 1. But sometimes  $N_{spp}$  comes out to be a fraction. In that case coil pitch is less than the pole pitch and the winding is said to be short-pitched. This design does not consider short pitched coils.

Along similar lines, the slot Pitch at Stator Inner Radius is found out to be:

$$\tau_s = R_{si} \theta_s \quad (3)$$

where Angular Slot-Pitch in mechanical radians is  $\theta_s = \frac{2\pi}{N_s}$

From this data, the slot and teeth dimensions can be determined as follows –  
Tooth Width is:

$$w_t = \tau_s - w_s \quad (4)$$

And Slot Bottom Width is given by:

$$w_{sb} = R_{sb} \theta_s - w_{tb} \quad (5)$$

NOTE: The dimensions of tooth are given by:

$d_s = d_1 + d_2 + d_3$ , where  $d_s$  is the tooth projection from the back iron core. The shoe of the tooth has height given by,  $d_1 + d_2 = \alpha_{sd} w_{tb}$ . The portion of the slot which houses a conductor is having a height  $d_3 = d_s - \alpha_{sd} w_{tb}$ .

When the teeth are parallel-sided a trapezoidal shaped slot area is achieved. It maximizes the winding area available and is used when the windings are to be wound turn-by-turn. On the other hand a parallel-sided slot design is used when the windings are formed prior to insertion into the slot. We have considered a trapezoidal slot here.

Once we achieve the dimensional details of slots and various radii, we can find out the slot cross sectional area available for conductors as:

$$A_s = d_3 \left[ \theta_s \left( R_{sb} - \frac{d_3}{2} \right) - w_{tb} \right] \quad (6)$$

[NOTE: Stator windings occupy this cross-sectional area, but due to insulations, slot-liners, etc. this entire area is not filled with conducting material. Hence a conductor packing factor needs to be defined as  $k_{cp} = \text{Area occupied by conductors} / \text{Total area}$ ]

Slot width just after the shoe portion of the tooth is:

$$w_{si} = (R_{si} + \alpha_{sd} w_{tb}) \theta_s - w_{tb} \quad (7)$$

where slot fraction is  $\alpha_s = \frac{w_{si}}{(w_{si} + w_{tb})}$

Total slot depth is given by:

$$d_s = R_{sb} - R_{ro} - g \quad (8)$$

#### *Magnetic parameters*

The flux path from rotor magnets-to-air gap-to-stator and back to rotor magnets shows that the machine can be modeled as one closed loop flux that repeats itself indefinitely. Flux from each magnet on rotor splits equally on both sides and couples to the two adjacent magnets. Thus we have a complete magnetic circuit with flux flowing through a number of reluctances such as rotor back iron, stator back iron, and air gap reluctance. The reluctances can be represented as permeances and parallel permeances are added. Expressions for the permeances in terms of geometric parameters are used to simplify the magnetic circuit. To find out the air gap flux density we need a magnet leakage factor, flux concentration factor, permeance coefficient and carter coefficient. These quantities are defined in terms of geometric as well fixed parameters as follows –

First, we have to take into account the irregularities introduced by the slotted design. This calls for a correction in air gap dimension. This correction is given by Carter Coefficient. For Carter Coefficient, the effective airgap is given by  $g_c = g + \frac{l_m}{\mu_r}$ .

Air-gap area is now given by:

$$A_g = \frac{(\tau_p)(L)(1+\alpha_m)}{2} \quad (9)$$

where  $\alpha_m$  is the magnet fraction defined as:

$$\alpha_m = (\text{Periphery covered by Magnets} / \text{Total Periphery})$$

Using the above data, we can arrive at the air gap flux density and hence the air gap flux,

$$B_g = \left[ \frac{C_\phi}{\left(1 + \frac{(\mu_r)(k_c)(k_{ml})}{P_c}\right)} \right] B_r \quad \text{and} \quad \phi_g = B_g A_g \quad (10)$$

This flux splits equally into both stator and rotor back irons and gets coupled to the adjacent magnets. Thus the back iron flux is given as,

$$\phi_{bi} = \frac{\phi_g}{2} \quad (11)$$

We know the maximum flux density  $B_{\max}$  allowed in the back iron from the fixed parameters. Using that, back iron width can be found out by:

$$w_{bi} = \frac{\phi_g}{2(B_{\max})(k_{st})(L)} \quad (12)$$

Now the air gap flux can also be used to determine the tooth width as we already know the maximum flux density allowed in the teeth. The air gap flux travels through the same number of teeth as the number of slots per pole. Using this we get the tooth width as:

$$w_{tb} = \frac{\phi_g}{(N_{sm})(B_{\max})(k_{st})(L)} = \frac{2w_{bi}}{N_{sm}} \quad (13)$$

Thus from the magnetic model, we have derived the construction details of the machine stator.

#### *Electrical Parameters*

Electrical parameters are a consequence of the geometric and magnetic design of the machine. The parameters resistances, inductances, current, EMF are all dependent on how the windings are. Machine ratings like the rated power, torque, speed, etc. dictate these parameters. The rated angular speed is determined from the desired frequency at which we want the machine to operate. The force produced by interaction of  $N_m$  magnet poles providing an air gap flux density of  $B_g$  with each pole interacting with  $n_s$  conductors, each carrying current  $i$  exposed over length  $L$  is given by:

$$F = (N_m)(B_g)(L)(N_{spp})(n_s)(i) \quad (14)$$

This force can be used to express machine torque in terms of the machine parameters already derived and assumed as fixed parameters as:

$$T = (N_m)(B_g)(L)(N_{spp})(n_s)(i)(R_{ro}) \quad (15)$$

When the number of slots per pole per phase is greater than one then a distribution factor comes into picture, which accounts for the reduction in the peak flux. A pitch factor also needs to be applied to the flux in that case. Also if the magnets are skewed, a skew factor is included as well. The final expression for torque becomes:

$$T = (N_m)(k_p)(k_d)(k_s)(B_g)(L)(N_{spp})(n_s)(i)(R_{ro}) \quad (16)$$

From the torque expression, the back emf is given as:

$$e_{\max} = \frac{T(w_m)}{i} = (N_m)(k_p)(k_d)(k_s)(B_g)(L)(N_{spp})(n_s)(R_{ro})(w_m) \quad (17)$$

This is the peak back emf at rated speed. This emf multiplied by the number of turns per slot gives the total emf.  $E_{\max}$ . This can lead us to find out the number turns per slot to be used to find out  $e_{\max}$ .

$$n_s = \text{int}\left[\frac{E_{\max}}{(N_m)(k_p)(k_d)(k_s)(B_g)(L)(N_{spp})(R_{ro})(w_m)}\right] \quad (18)$$

This truncated value of number of turns per slot is used to find out the actual emf resulting from the design. The number of turns per slot also gives the total slot current,

$$I_s = \frac{T}{(N_m)(k_p)(k_d)(k_s)(B_g)(L)(N_{spp})(R_{ro})} \quad (19)$$

This slot current gives us the knowledge of the slot current density, as we already know the slot area. If this value exceeds the maximum permissible current density  $J_{\max}$  then, the slot area has to be increased by changing the stator outer radius and rotor outer radius. Once the slot current is obtained, one can deduce the expression for phase current since the total number of slots and the number of phases are known.

$$I_{ph} = \frac{I_s}{(N_{ph})(n_s)} \quad (20)$$

### PM Machine Design Results

The machine performance is observed in terms of the efficiency, torque, losses, and phase currents against the variation in the operating frequency. Keeping in mind that the frequency of the machine will dictate the size, we obtained the desired results at 60Hz, 400Hz, 800Hz and 1200Hz. The results show a similar trend in the variation. However, one important thing to note is the impact of some of the assumptions that are made initially. Certain assumptions are critical to the overall performance of the machine. One set of assumptions which were visibly very dominant in dictating the performance was  $K_e$  (Eddy current constant for the core material) and  $K_h$  (Hysteresis constant for the core material). A small change in the values of these constants implies a large change in the efficiency of the machine. This is because these constants are responsible for determining the losses in the machine. The variation in efficiency of machine versus the change in these constants is shown in Figs. 4 and 5. A comparison of machine parameters for varying frequencies is presented in Table 2.

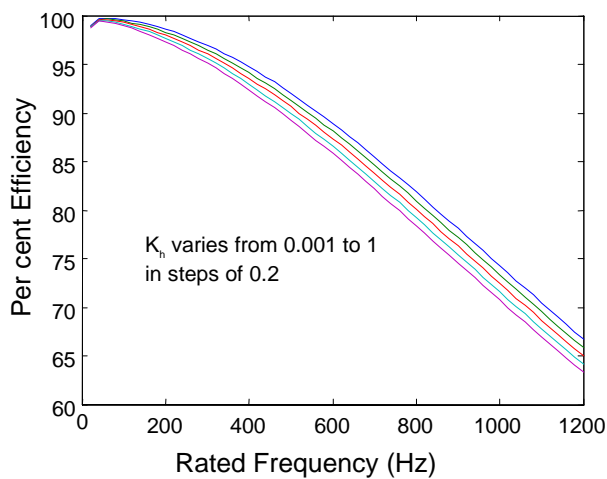


**FIGURE 4.** Variation in Efficiency as a Function of Frequency as Well as  $K_h$ .

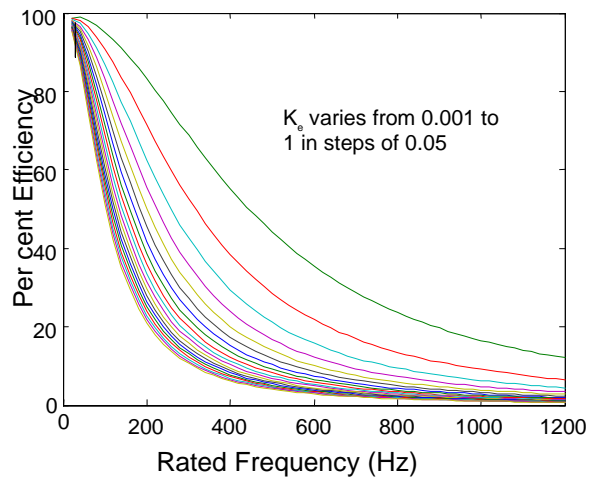


**FIGURE 5.** Variation in Efficiency as a Function of Frequency as Well as  $K_e$ .

**TABLE 2.** Machine Comparisons at Different Frequencies.

| Operating Frequency (Hz)              | 60    | 400    | 600    | 800    | 1000   |
|---------------------------------------|-------|--------|--------|--------|--------|
| Power Output ( $W_e$ )                | 458   | 19206  | 41687  | 71508  | 107590 |
| Input Power Required ( $W_e$ )        | 538.2 | 19940  | 44828  | 77730  | 115904 |
| Total Losses ( $W_e$ )                | 80.14 | 733.43 | 3140.9 | 6222.2 | 8314.0 |
| Core Losses ( $W_e$ )                 | 59.97 | 706.34 | 3105.5 | 6175.8 | 8254.3 |
| Copper Losses ( $W_e$ )               | 0.169 | 7.0877 | 15.384 | 26.389 | 39.704 |
| Efficiency (%)                        | 85.1  | 96.321 | 92.993 | 91.995 | 92.827 |
| RMS Phase Current (A)                 | 9.09  | 63.897 | 94.137 | 123.29 | 151.23 |
| Armature Current Density ( $A/mm^2$ ) | 0.058 | 0.3761 | 0.5541 | 0.7257 | 0.8901 |
| Stator Teeth Flux Density (T)         | 0.83  | 0.8305 | 1.3380 | 1.5649 | 1.5650 |

### CONCLUSION

Terrestrial and aircraft power system architectures are two of the most successful applications of engineering innovation and ingenuity that are at the core of the comforts and conveniences of modern living. Incredibly, the technological challenges in building power systems for future space exploration and habitation on the Moon or Mars will be multiplied many fold.



As compared to terrestrial applications, the requirements of modularity, fault tolerance, protection and safety, reserve power and emergency backup requirements, power and energy density, etc. all have to be higher. However, much of the existing technology may be retooled, and in some case, enhanced to get them close to match the requirements of the proposed new space explorations. This study clearly points out the fact that as we opt for higher operating frequencies, the machine is able to deliver more power for the same dimensions. However, there beyond a certain operating frequency, the input power has to be increased. This will most likely dictate the choice of a prime mover. The variation in the size of the machine will directly affect the magnetic flux density and the magnetic flux existing in the machine. Power electronics will continue to dictate much of the distribution of electric power both on board the space exploration vehicle as well as for the habitat on lunar or Martian surface. High reliability dictates the need for redundancy and the combined use of AC/DC systems.

## NOMENCLATURE

|                                       |  |  |
|---------------------------------------|--|--|
| $k_c$ = Carter coefficient            | $k_{ml}$ = Magnet leakage Factor                 | $B_r$ = Magnet remnance (T)                  |
| $\mu_R$ = Magnet recoil permeability  | $P_c$ = Permeance coefficient                    | $w_{tb}$ : Tooth bottom width (m)            |
| $R_{st}$ : Stator inside radius (m)   | $\theta_p$ : Angular span of one pole of machine | $\phi_g$ : air gap flux (Wb/m <sup>2</sup> ) |
| $\alpha_p$ : Pitch factor             | $N_{spp}$ : Number of slots per pole per phase   | $l_m$ : Magnet Length (m)                    |
| $N_s$ : Total number of slots         | $R_{sb}$ : Radius at the slot bottom (m)         | $C_\phi$ : Flux concentration factor         |
| $\alpha_{sd}$ : shoe depth fraction   | $g$ : Air gap length (m)                         | $B_g$ : Air gap flux density (T)             |
| $k_{st}$ : Lamination stacking factor | $N_{sm}$ : Number of slots per magnet pole       |  |

## ACKNOWLEDGMENTS

This work was supported in part by the NASA Johnson Space Center and the American Society of Engineering Education.

## REFERENCES

- Algen, O., "Loss Calculation and Thermal Analysis of a High-speed Generator," in Proceedings of 2003 *IEEE International Electric Machines and Drives Conference (IEMDC'03)*, vol. 2, 2003, pp. 1117 – 1123.
- Caricchi, F., Crescimbin, F., Honorati, O., Bianco, G. L., and Santini, E., "Performance of Coreless-Winding Axial-Flux Permanent Magnet Generator with Power Output at 400Hz, 3000 r/min," *IEEE Transaction on Industry Applications*, **34**, 1263-1269 (1998).
- Deshpande, U.S. "Recent Advances in Materials for Use in Permanent Magnet Machines – A Review," in Proceedings of 2003 *IEEE Int'l Electric Machines and Drives Conference*, vol. 1, 2003, pp. 509-515.
- Dravid, N., "Performance Prediction for a Permanent Magnet Two-pole Synchronous Machine for a Flywheel Energy Storage System," *Aerospace Power and Electronics Workshop*, 2003, pp. 611-616.
- Hendershot, J.R. and Miller, T.J.E., *Design of Brushless Permanent-Magnet Motor*, Magna Physics Publishing and Clarendon Press, Oxford, 1994, pp. 126-152.
- Henselman, D.C., *Brushless Permanent-Magnet Motor Design*, McGraw-Hill, New York, 1994, pp. 280-299.
- Huang, S., Luo, J., Leonardi, F. and Lipo, T., "A General Approach to Sizing and Power Density Equations for Comparison of Electrical Machines," *IEEE Transaction on Industry Applications*, **34**, 92-97 (1998).
- Magnussen, F., Chin, Y. K., Souldard, J., Broddefalk, A., Eriksson, S., and Sadarangani, C., "Iron Losses in Salient Magnet Machines at Field-weakening Operation," in Proceedings of 2004 *Ind. App. Conf.*, vol. 1, 2004, pp 40-47.
- Mi, C. C., Slemon, G. R., and Bonert, R., "Minimization of Iron Losses of Permanent Magnet Synchronous Machines," *IEEE Transaction on Energy Conversion*, **20**, 121-127 (2005).
- Nagorny, A., "High Speed Permanent Magnet Synchronous Motor/Generator Design for Flywheel Applications," (2004) <http://www.ansoft.com/workshops/aeroec04/Nagorny.pdf>, accessed 05/08/2005.
- Ojo, O., Cox, J., and Wu, Z., "Permanent Magnet Machines," *IEEE Transaction on Energy Conversion*, **12**, 351-356 (1997).
- Qu, R., and Lipo, T. A., "Design and Parameter Effect Analysis of Dual-Rotor, Radial Flux, Toroidally Wound, Permanent Magnet Machines," *IEEE Transactions on Industry Applications*, **40**, 771-779 (2004).
- Sahin, F., Vandenput, A.J.A., and Tuckey, A.M., "Design, Development and Testing of High-speed Axial-Flux Permanent-Magnet Machine," in Proceedings of 2001 *Ind. App. Conf.*, vol. 3, 2001, pp. 1640 – 1647.
- Trout, S. R., and Wooten, G. D., "Selection and Specification of Permanent Magnet Materials," in Proceedings of *Electrical Insulation Conference and Electrical Manufacturing and Coil Winding Technology Conf.*, 2003, pp. 59-63.

Copyright of AIP Conference Proceedings is the property of American Institute of Physics and its content may not be copied or emailed to multiple sites or posted to a listserv without the copyright holder's express written permission. However, users may print, download, or email articles for individual use.